Meshfree Method To Predict The Effect of Corrugated Bed on Hydraulic Jump Characterictic Especially Energy Dissipation

Syamsuri[1,a] and Tungga Bhimadi[1, b]

[1]Department of Mechanical Engineering Adhi Tama Institute of Technology Surabaya, Indonesia

[a]syam_sby2003@yahoo.com, [b]tunggabhimadi@yahoo.com

Keywords: Hydraulic jump, smoothed particle hydrodynamics model, energy dissipation, and effect of corrugated beds.

Abstract. A hydraulic jump is a common phenomenon which can be observed in open channels flow such as rivers and spillways. It can cause damage of the downstream bed and bank of the channel due to the process of continuous erosion and degradation. In order to reduce the hydraulic jump destruction, the energy in the hydraulic jump must be dissipated as much as possible. One method to increase dissipation of energy is using a corrugated bed. In order to know the effect of a corrugated bed on the hydraulic jump, a smoothed particle hydrodynamics (SPH) model is applied to investigate the characteristics of hydraulic jumps in various corrugated beds. A variety of corrugated beds which are smooth, triangular, trapezoidal, and sinusoidal are considered. The opening of a gate is changed to adjust the hydraulic jump. The energy dissipation are reported. The results of the present study are in a good agreement with previous studies. Energy dissipation is compared among corrugated beds and a smooth bed. It is found that the sinusoidal bed can dissipate more energy than other beds. As a result, corrugated beds can be used to enhance energy dissipation of hydraulic jump in the open channel. In general, the proposed SPH model is capable of simulating the effect of corrugated beds on hydraulic jump characteristics. This template explains and demonstrates how to prepare your camera-ready paper for *Trans Tech Publications*. The best is to read these instructions and follow the outline of this text.

Introduction

A hydraulic jump in a horizontal channel with a smooth bed has been studied extensively by many researchers such as [37] and [29]. Recently, a number of studies regarding hydraulic jumps have been carried out on rough and corrugated beds. However, the main concern with hydraulic jumps on rough and corrugated beds is that the roughness elements and crest of corrugations might be subjected to cavitation and erosion. Therefore, cavitation and erosion may damage the structure itself. Ead et al [15], showed that if the crests of corrugations are placed at the upwind side carrying the supercritical flow, the corrugations will not protrude into the flow and then preventing cavitation in the basin. Furthermore, they also reported that, in culvert with corrugated bed, Reynolds shear stress was produced so that the velocity magnitude above the corrugations was reduced.

Ead and Rajaratnam [14], studied hydraulic jumps on a corrugated bed experimentally in the range of Froude numbers from 4 to 10. Three relative roughnesses tc/y1 (tc is the height of corrugations and y1 is the initial depth of flow); 0.50, 0.43, and 0.25, were studied. They found that the reduction of the jump forming tailwater depth was due to the interaction between the supercritical stream and the bed corrugations. Tokyay [36], investigated the effect of channel bed corrugations on a hydraulic jump experimentally. In the experiments, two wave steepnesses, 0.20 and 0.26, were used and the range of Froude numbers varied from 5 to 12. The results showed that many factors, such as initial depth of flow, supercritical Froude number, height and wave length of corrugations were effective on the characteristics of the hydraulic jump.

Gharangik and Chaudhry [18], investigated a hydraulic jump using a numerical model. They applied the Boussinesq equations to simulate both the sub and supercritical flows and a hydraulic jump in a rectangular channel with an inclined bed. The numerical study of a hydraulic jump on a smooth bed has also been carried out by [39], . They used the volume of fluid (VOF) and the

turbulence model to predict the surface elevation for the hydraulic jump and horizontal velocity downstream of the jump. Sarker and Rhodes [32], studied a hydraulic jump on a smooth bed by experimental and numerical methods. They used the RNG κ−_ turbulence model in combination with the volume of fluid (VOF) method for free surface modeling. There was a good agreement in the prediction of the free surface hydraulic jump between the two-dimensional numerical solution and the experimental measurements. The finite volume TVD-MacCormack scheme for the computation of two-dimensional open channel flows with abrupt changes has also been studied by [7]. This scheme was robust and stable in capturing strong gradient and discontinuities in open channel flows like an oblique hydraulic jump, a circular dam break and two dimensional dam break.

On the other hand, instead of the mesh-based viewpoint of the simulation domain, meshless methods adopt a particle view throughout the problem domain. One distinct meshless particle method is smoothed particle hydrodynamics (SPH). SPH provides some advantages in comparison with the usual limitations of Eulerian mesh-based methods. Liu and Liu [21], mentioned that SPH conserves mass exactly and has the strong capability to deal with free surface and moving interface problems . Thus, it is suitable for modeling dam break flows. Standard SPH is formulated for solving the Navier-Stokes equations from [25]. Recently, there has been significant progress in the applications of standard SPH to dam-break behavior modeling. Most of them targeted on 2D coastal flow simulations, fluid-structure interaction [28], wave generation from [38], and wave breaking from [39]. For practical engineering applications, i.e., hydraulic jump, only few studies have attempted to investigate this topic. Lopez et al. [22], found that SPH provided good average pressures values at the bottom of the basin in the jump influence area, but large dispersion was observed for instantaneous water height values. It was considerably improved by introducing another turbulence model. An extensive validation in comparison with experimental results was investigated by [6]. A meshless numerical model was proposed to solve the shallow water equation (SWE) for dam break flows in 1D and 2D open channels based on smoothed particle hydrodynamic in Chang et al.'s study [6]. They used three benchmark problems including dam break flows through a rough flat channel, a rough bumpy channel with various downstream boundary conditions and a nonprismatic channel as 1D problems. A realistic scale model of the Toce river in Italy was used for 2D problems. The SPH simulated results indicated that accurate performance was reached in the presence of shock discontinuities, shock front motion and hydraulic jumps. Federico et al. [17] proposed a particular initial configuration that has been adopted to keep the jump close to its initial position and to avoid the use of any weir downstream. Various jumps have been simulated at a number of Froude numbers.

Although some investigations have recently been carried out on hydraulic jumps on corrugated bed, the information regarding the effects of corrugation on hydraulic jump characteristics is incomplete. The objective of this research is to investigate the effect of smooth, triangular, trapezoidal, and sinusoidal beds on the characteristics of a jump using SPH method.

ISPH Formulae for Incompressible Fluid Flow

SPH is an interpolation method which allows a function to be expanded in terms of its values at a group of disordered particles from [25]. The fundamental principle is to approximate a continuous function $A(\mathbf{r})$ by:

$$A(r) = \int A(r')w(r - r', h)\,dx' \tag{1}$$

where **r** is the displacement vector, *h* is called the smoothing length and w(**r** - **r'**, h) is the weighting function or kernel. For numerical implementation, the integral interpolant is approximated by the summation interpolant:

$$A(r) = \sum_b m_b \frac{A_b}{\rho_b} w_{ab} \tag{2}$$

where the summation is over all the neighboring particles. ρ_b and m_b are density and the mass of a particle, respectively. $w_{ab} = w(r_a - r_b, h)$ is weighting or kernel function.

Governing equations for viscous fluid motion, which are momentum and mass conservation equations, can be presented in the followings:

$$\frac{Dv}{Dt} = -\frac{1}{\rho}\nabla P + g + \nu_o \nabla^2 v \tag{3}$$

and

$$\frac{1}{\rho}\frac{D\rho}{Dt} + \nabla . v = 0 \tag{4}$$

where **v** is the velocity vector, P is the pressure, **g** is acceleration due to gravity and $\upsilon_0 \nabla^2 v$ refers to the diffusion terms.

In conventional SPH notation of momentum and mass equations, artificial viscosity is used (see Dalrymple and Rogers (2006)):

$$\frac{Dv_a}{Dt} = -\sum_b m_b \left(\frac{P_b}{\rho_b^2} + \frac{P_a}{\rho_a^2} + \Pi \right) \nabla_a w_{ab} + g \tag{5}$$

and

$$\frac{D\rho_a}{Dt} = -\sum_b m_b v_{ab} \nabla_a w_{ab} \tag{6}$$

In the above equations, $\nabla_a w_{ab}$ is the gradient of the kernel with respect to the position of particle a. P_k and ρ_k are pressure and density of particle k (evaluated at a or b)

$$\Pi_{ab} = \begin{pmatrix} \dfrac{-\alpha \bar{c}_{ab} \mu_{ab}}{\bar{\rho}_{ab}} & v_{ab} r_{ab} < 0 \\ 0 & v_{ab} r_{ab} > 0 \end{pmatrix} \tag{7}$$

where α is an empirical coefficient, $\bar{c}_{ab} = (c_a + c_b)/2$, $\bar{\rho}_{ab} = (\rho_a + \rho_b)/2$ and $\mu_{ab} = \dfrac{h v_{ab} r_{ab}}{r^2_{ab} + 0.01h^2}$.

The parameter α must be given properly for a stable and accurate solution. In most of cases, α is of the order 10^{-2} for free surface flows of Colagrossi [8]. A large value of α would delay the wave breaking phenomena as shown in [12].

In general, the accuracy of the SPH interpolation increases with the order of the polynomial used in the weighting function of Capone *et al.* [5]. The quintic kernel can be a good choice since it provides a higher order of interpolation. In the present study, we use the quintic kernel function from multifarious possible kernel.

$$w_{ab} = w(r_a - r_b, h) = \alpha_N \left(1 - \frac{q}{2}\right)^4 (2q+1) \quad 0 \le q \le 2 \tag{8}$$

where $q = r_{ij}/h$ and $\alpha_N = \dfrac{7}{4\pi h^2}$. The tensile correction is automatically activated when using kernels with first derivatives that go to zero with decreasing inter-particle spacing. In addition, particles are moved with the following equation:

$$\frac{dr_a}{dt} = v_a + \varepsilon \sum_b m_b \left(\frac{v_a - v_b}{\rho_a} \right) w_{ab} \tag{9}$$

The last term including the parameter $\varepsilon = 0.5$ is the so-called "XSPH correction" proposed by [23]. It ensures that neighboring particles move with approximately the same velocity. This prevents particles with different velocities occupying nearly the same location.

The equation of state allows us to avoid expensive computation of the Poisson's equation for pressure, but it inverts any incompressible fluids to be weakly compressible from [11]. The equation of state relates the pressure of the fluid to the local density and is denoted as

$$P = B\left[\left(\frac{\rho}{\rho_o}\right)^{\gamma} - 1\right] \tag{10}$$

Herein, $\gamma = 7, \mathrm{B} = c_0^2 \rho_0 / \gamma$ and c_0 is the speed of sound. The reference density ρ_0 is 1000 kg/m^3 in this study. Based on the speed of sound in water, a very small time step must be adopted for numerical modeling according to the Courant-Fredrich-Levy condition. Nevertheless, the speed of sound should be about ten times faster that the fastest fluid velocity in order to let the change in fluid density be less than 1% [11] so that the transient simulation can be stable.

Artificial viscosity which originally was used in the equation of motion has a few advantages and disadvantages. First of all, it can stabilize a numerical scheme in free surface problems. Secondly, artificial viscosity prevents particles from interpenetrating with each other [11]. Subsequently, it preserves both linear and angular momentum and has an acceptable manner in the case of rigid body rotation, see [23]. In contrast, the artificial viscosity has some disadvantages. It is a scalar viscosity which cannot take the flow direction into account [20]. so it causes strong dissipation and affects shear stress in the fluid flow, see [11]. Thus, researchers prefer to simulate viscosity in a realistic manner [11].

One realistic expression of viscosity is the molecular viscosity [26]. It causes shear stress in a laminar flow while a velocity gradient exists. In a turbulent flow, additional stress is generated due to eddy motion. The Sub-Particle Scale (SPS) technique is used to model turbulence in the present study. The SPS approach to model turbulence is also employed in other particle methods such as MPS [19] and Incompressible SPH [34]. Recently, Dalrymple and Rogers [12], implemented this expression of SPS viscosity in the compressible SPH method. We used the molecular viscosity and Sub-Particle Scale (SPS) turbulence model in this study. Implementation of SPS approach in the diffusion term of momentum equation (Eq. (3)) gives:

$$\frac{Dv}{Dt} = -\frac{1}{\rho}\nabla P + g + \nu_o \nabla^2 v + \frac{1}{\rho}\nabla \tau \tag{11}$$

where υ represents the molecular viscosity and τ represents SPS stress tensor which was modeled by the eddy viscosity. Dalrymple and Rogers (2006) gave the momentum equation [Eq. (11)] in SPH notation using molecular viscosity and SPS turbulence model for a fluid particle *a*:

$$\frac{Dv_a}{Dt} = -\sum_b m_b \left(\frac{P_b}{\rho_b^2} + \frac{P_a}{\rho_a^2} + \Pi\right)\nabla_a w_{ab} + g + \sum_b m_b \left(\frac{4\nu_o v_{ab} r_{ab}}{\left|r_{ab}^2\right|(\rho_a + \rho_b)}\right)\nabla_a w_{ab} + \sum_b m_b \left(\frac{\tau_b}{\rho_b^2} + \frac{\tau_a}{\rho_a^2}\right)\nabla_a w_{ab} \tag{12}$$

where υ_0 is the kinetic viscosity of laminar flow (10^{-6} m^2/s in this study).

While the results obtained by SPH simulations are generally reasonable, the pressure field of the particles exhibits large oscillations. Efforts to overcome this pressure oscillating problem have been concentrated on several approaches including correcting the kernel (for an overview, see [2] and developing an incompressible solver. One of the most straight forward and computationally least expensive ways is to perform a filter over the density of the particles and the re-assign a density to each particle, see [8]. There are two ways of correction, zeroth order and first order.

The Moving Least Squares (MLS) approach was developed by [13] and successfully applied to free surface problems by [8] and [30]. It is a first-order correction so that the variation of a linear density field can be exactly reproduced by

$$\overline{\rho}_a = \sum_b \rho_b \, w_{ab}^{MLS} \frac{m_b}{\rho_b} = \sum_b m_b \, w_{ab}^{MLS} \tag{13}$$

The corrected kernel is evaluated as follows

$$w_{ab}^{MLS} = w_b^{MLS}(r_a) = \beta(r_a).(r_a - r_b)\, w_{ab} \tag{14}$$

so that in 2-D

$$w_{ab}^{MLS} = [\beta_o(r_a) + \beta_{1x}(r_a)(x_a - x_b) + \beta_{1z}(r_a)(z_a - z_b)]w_{ab} \tag{15}$$

where the correction vector β is given by

$$\beta(r_a) = \begin{pmatrix} \beta_o \\ \beta_{1x} \\ \beta_{1z} \end{pmatrix} = A^{-1} \begin{pmatrix} 1 \\ 0 \\ 0 \end{pmatrix} \tag{16}$$

where

$$A = \sum_b w_b(r_a) \, \overline{A} \frac{m_b}{\rho_b} \tag{17}$$

with the matrix $\overline{A}$ being given by

$$\overline{A} = \begin{pmatrix} 1 & (x_a - x_b) & (z_a - z_b) \\ (x_a - x_b) & (x_a - x_b)^2 & (z_a - z_b)(x_a - x_b) \\ (z_a - z_b) & (z_a - z_b)(x_a - x_b) & (z_a - z_b)^2 \end{pmatrix} \tag{18}$$

More regular density distribution can be obtained using the MLS density filter, see [10]. The MLS density filter is used in this study.

Numerical Model

A hydraulic jump is a type of shock wave where the flow undergoes a sudden transition from swift, thin (shallow) flow to tranquil, thick (deep) flow. Hydraulic jumps are well-known in the context of open-channel flows. Hydraulic jumps in open-channel flow are characterized as a drop in Froude number F_1 defined as

$$F_1 = \frac{v}{\sqrt{g\, y}} \tag{19}$$

from supercritical ($F_1 > 1$) to subcritical ($F_1 < 1$) conditions. The result is a piecewise increase in depth y and a step decrease in flow velocity v passing through the jump.

The depth of supercritical flow, y_1, ”jumps” up to its subcritical conjugate depth, y_2, and the result of this abrupt change in flow conditions is considerable energy loss and turbulence, E_L. Fig. 1 shows a schematic of typical jump characteristics where E_1 is the energy of the upstream flow, E_2 is the energy of the downstream flow and Lj is the length of the hydraulic jump. A series of small surface rollers are formed in a standing wave like the one shown in Fig. 1.

Fig. 2 shows the schematic of the model for validation. A water bowl is utilized at the tank in order to decrease its volume, to diminish the number of particles, and to reduce the computational time. For this test, the Froude number of the flow upstream of the jump is around 3.5. The same viscosity model is used for both validation and application models. In this study SPS turbulence model for viscosity is applied. Fluid particles are initially placed in a staggered grid with the particle spacing dx = dz = 0.2 m.

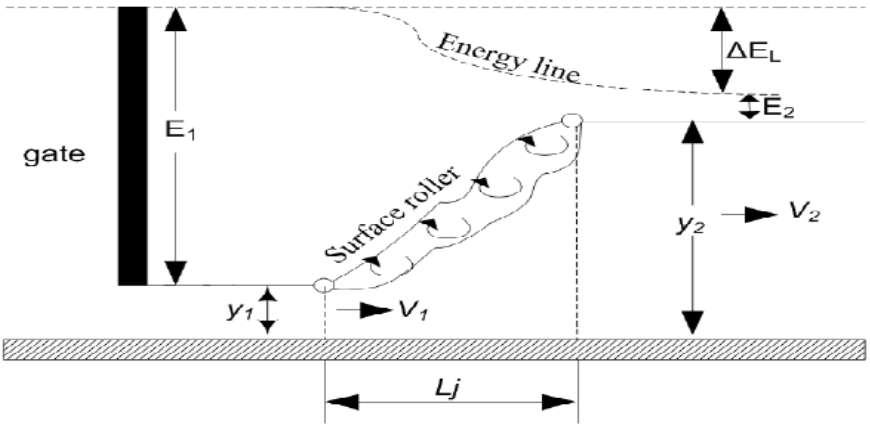

Fig 1. Schematic of hydraulic jump

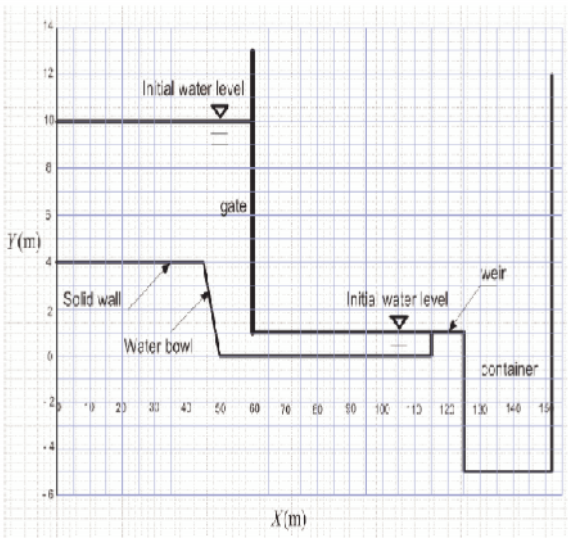

Fig 2. Sketch of the tank

Details of the Basin

The numerical model is applied and the primary numerical details for different corrugated beds are shown in Fig. 3. A hydraulic jump is produced in a rectangular flume which is 1 m deep and 60 m long. A weir crest is not installed in this model. Corrugated sinusoidal sheets, corrugated triangular sheets and trapezoidal sheets (see Fig. 3) are installed on the flume bed in such a way that the crests of corrugations are at the same level as the upstream bed where the supercritical stream is produced by a sluice gate. The corrugations act as depressions in the bed and create numerous turbulent eddies which might increase the shear stress on the bed surface. All the three types of corrugations have a wavelength s of 0.19 m in the flow direction and an amplitude t_c of 0.19 m, according to [16] study where $t_c/y_1 = 0.36$, $s = t_c$, and $\theta = 45^0$ are used. t_c/y_1 is defined as the ratio of the amplitude of the corrugation to the initial depth. One of the two trapezoidal sections and the triangular

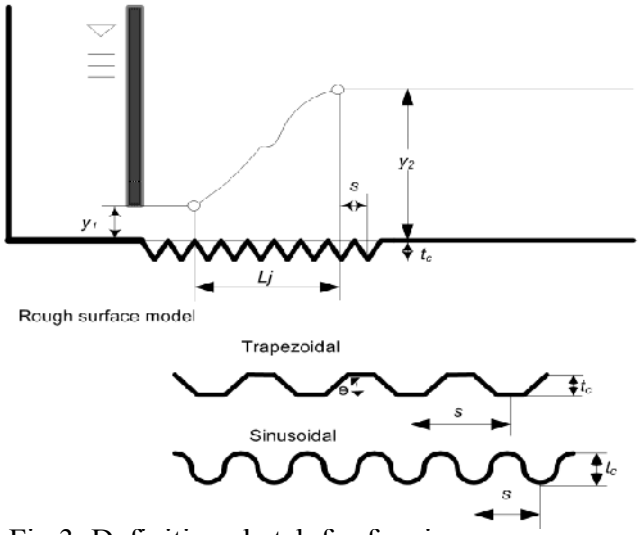

Fig 3. Definition sketch for free jumps on corrugated beds

section have the slope of 45 degrees. The discharge is 10.96 m^3/s. Water enters the flume under a sluice gate with a streamlined lip, producing a uniform supercritical stream with a thickness of y_1. A tailgate is used to control the tailwater depth in the flume. In this study, the tailgate is adjusted so that the jumps are formed on the corrugated beds (see Fig. 3).

The initial depth y_1 measured above the crest level of corrugations on the plane bed is equal to 1.76, 1.618, 1.45, 1.252, 1.109, 0.846, 0.788, 0.698, and 0.63 for different Froude numbers. Values of y_1 and V_1 are selected to achieve a wide range of the Froude numbers from 1.5 to 7.0. The Reynolds number $Re = V_1 y_1/\nu$ varies from 6.90E6 - 1.095E7.

Initial Condition and Boundary Condition

The initial condition is designed to fit the experimental conditions undertaken by Lopez *et al.* (2010). The present computational system consists of fluid particles and walls. The still water depth is 10 m. The opening of the gate is 1 m. The crested weir is 1 m high. The basin is 115 m long. Froude number in this case is around 3.5. The total number of particles in the numerical model is 22,000 (including 2,723 boundaries particle). Another study uses 11,000 particle to simulate this problem, see [22].

In this study, the gate and the bottom boundary such as smooth, triangular, trapezoidal, and sinusoidal are defined by lines of particles that exert repulsive forces on fluid particles (for the similar idea, see [31]. It is natural to choose central forces similar to those in molecular dynamics from [24], but they produce the equivalent of a corrugated boundary with ripples on the scale of the particle spacing.

Boundary particles are distributed evenly (along the boundary) and have a local unit normal vector **n** that points from the boundary into the fluid. The force per unit mass fak on a fluid particle from a boundary particle is computed using the components of their separation along the normal (denoted below by y) and along the tangent (x). The distances x and y are taken as positive. The force then takes the form

$$f_{ab} = \mathbf{n}\, R(y)\, P(x), \tag{20}$$

where R(y) is designed to fall to zero within a few particle spacings of the wall. Also, P(x) is designed to ensure that as a fluid particle moves between two boundary particles. The contributions from the particles will combine to make the boundary force constant if the fluid particle moves parallel to the boundary.

Fixed solid particles are allocated in the two rows to form a staggered grid with dx = dz = 0.1 m and zero initial velocity. Their positions remain unchanged during the numerical simulation ($V^{solid}(t) = 0$ and $r^{solid}(t) = r^{solid}(0)$).

Results and Discussion

First, we consider an experimental case previously investigated by [22] and shown in Fig. 2. 22, 000 particle are used in this case. The initial condition given by [22] is described in initial conditions

and boundary conditions. The simulation is performed in a workstation with two 3.40GHz Intel CPU and 3GB RAM. It takes less than 72 CPU hours to compute results up to the total time of 20 sec.

Table 1 summarises the characteristic parameters for a mobile hydraulic jump: the initial depth (y_1), velocity (v_1), Froude number (F_1), location of the jump front (X_{in}), and conjugate depth (y_2). The last three columns in Table 1 compare the analytical conjugate depth and is given by the well-known Belanger's equation

$$y_2 = \frac{y_1}{2}\left(\sqrt{(1+8F_1^2)} - 1\right) \tag{21}$$

This equation is applied only to a flat bed. The reason for this discrepance between analytic and numerical solutions may be the inviscid or frictionless flow assumption which means that viscous effect and sidewall friction in Eq. (21) is ignored along the bed in the analytic solution.

Table 1: Results for validation.

Time (s)	y_1 (m)	v_1 (m/s)	F_1	y_2 (analytic) (m)	y_2 (SPH1) (m)	y_2 (SPH2) (m)
5	0.84	10.30	3.59	3.87	3.08	3.10
10	0.80	10.05	3.58	3.68	3.52	3.53
15	0.80	10.03	3.6	3.71	3.70	3.72
20	0.78	9.29	3.36	3.34	3.35	3.38

Notes:

Artificial viscosity is used in SPH1.

SPS turbulence model for viscosity is used in SPH2.

It is important that the value of y_2 should be approximately constant in order to get a qualitative result. The variation of y_2 with time is shown in Fig. 4. The steady condition is reached after 10 seconds.

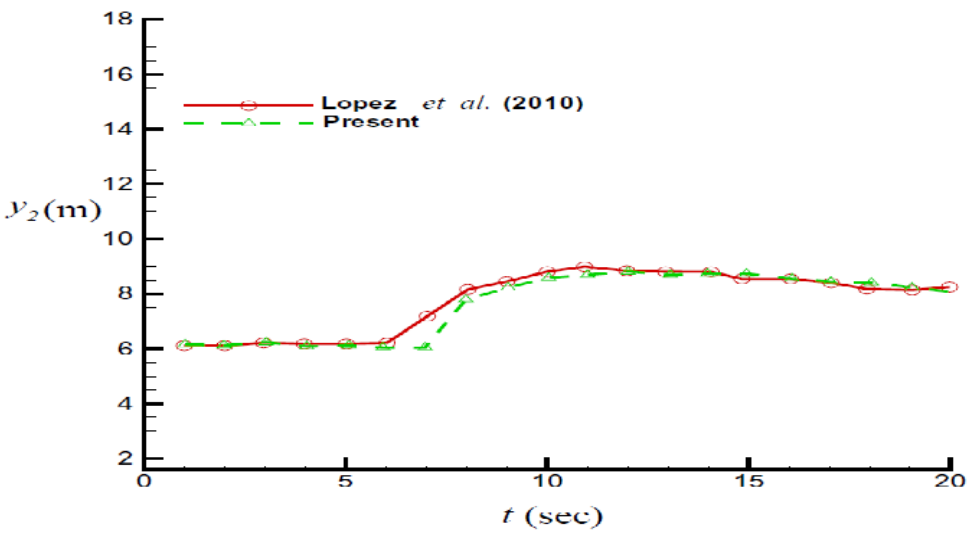

Fig 4. The comparison of y_2 with time (t) between experimental, by Lopez et al.(2010) and present study.

Fig. 5 shows the comparison between numerical and experimental free surface profiles provided by Lopez [22] at successive time steps. While the gate is open, fluid particles flow into the basin. This flow gives rise to a mobile hydraulic jump that travels downstream. The water level at point A is lower than the depth of the jump at point B. It happens 5 seconds after the gate is opened. This surface

profile looks like a ”crown” shape. After 10 sec, the wave arrives in front of the weir and generates a critical section that imposes a higher free surface level of the jump. A wave of higher elevation is evident in the area surrounding the weir. Afterwards, this wave propagates to the downstream direction and then the hydraulic jump remains constant. This happens at t = 15 sec. The hydraulic jump reflected by the weir returns upstream and arrives in the front of the jump at t = 20 sec. The lower flow velocity caused by the decrease in reservoir level forces the jump to return upstream. The numerical prediction is in a satisfactory agreement with the experimental results.

The energy dissipation of the jump

One of the most important engineering applications of the hydraulic jump is energy dissipation in channels, dam spill ways and similar structures, so that the excess kinetic energy does not damage these structures. The rate of energy dissipation or head loss across a hydraulic jump is a function of F_1. The head loss increases with the increase in F_1 from [4].

The efficiency of the hydraulic jump η , can be expressed as $100\%-(E_1 - E_2)/E_1$, where $E_1 = y_1 + Q^2/(2gy_1)$ and $E_2 = y_2 + Q^2/(2gy_2)$ are the energy before and after the jump, respectively. In Fig. 6, the relative energy loss E_L/E_1 is plotted versus

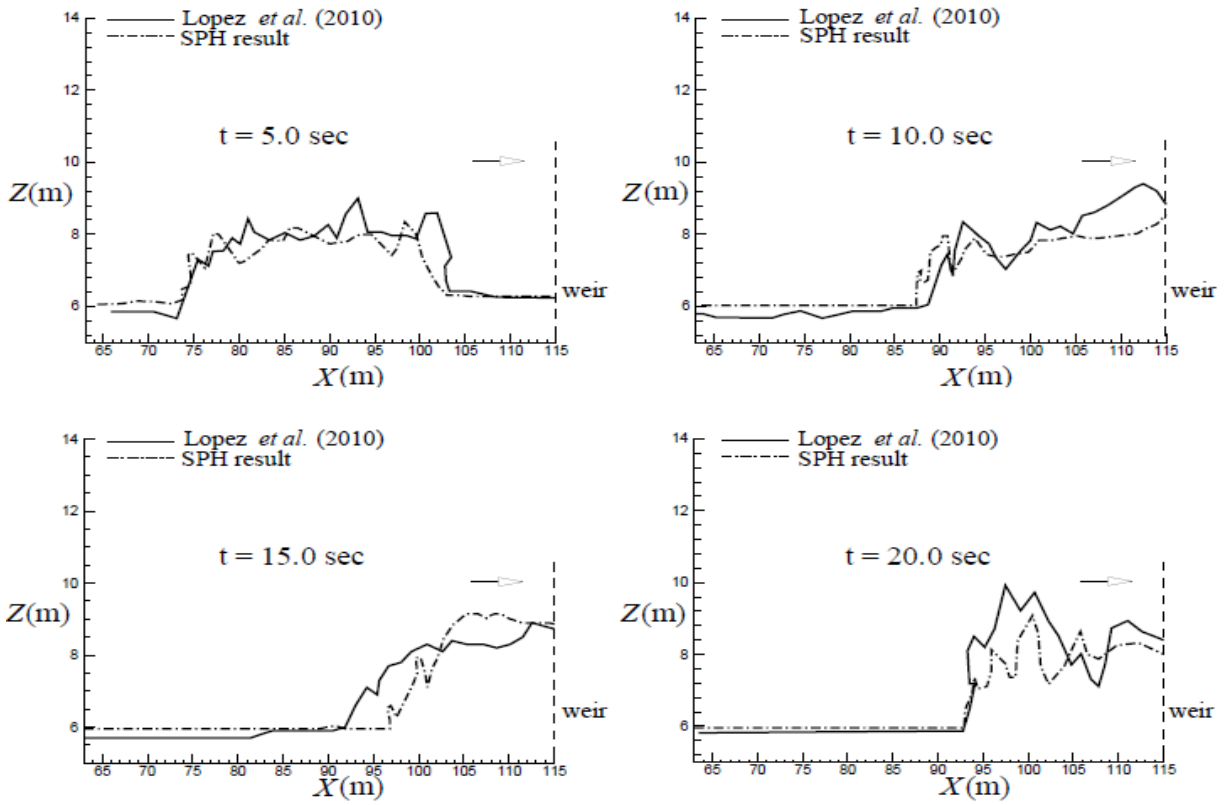

Fig 5. The comparison of surface profile of hydraulic jump at t = 5.0 sec, t = 10.0 sec, t = 15.0 sec, and t = 20.0 sec

different Froude numbers where $E_L = E_1 - E_2$. Figure 6 indicates that when the Froude number increases, the energy dissipation of the hydraulic jump also increases since the energy dissipation is a function of Froude number, see [4]. Fig. 6 also shows that for similar Froude numbers, the energy loss of a jump on a corrugated bed is higher than that on a smooth bed. The findings of the current study are consistent with [14] who mentioned the same result and trend. The difference between the energy dissipation for jumps on the sinusoidal bed and the smooth bed is about 22% for F_1 less than 5.0. On the other hand, when the F_1 is larger than 5.0 the difference of energy dissipation of the smooth and sinusoidal bed is less than 2.5%.

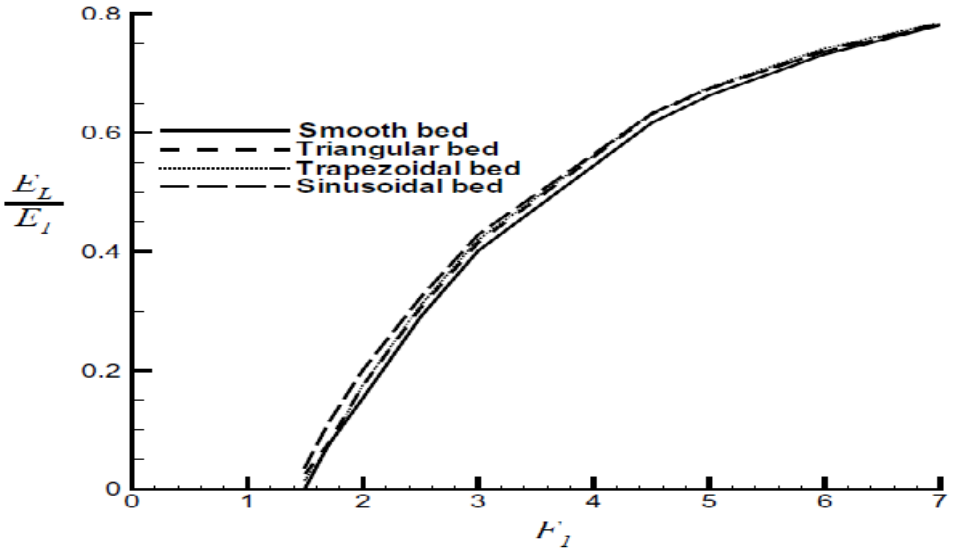

Fig 6. Relationship between percentage of energy dissipation and Froude numbers.

In addition, Fig. 7 shows the time histories of specific energy for different beds. Using the equation of specific energy $Es = y_2 + Q^2/(2gy_2)$, it shows that specific energy for a sinusoidal bed is lower than others. The reason for the reduction of specific energy is the enhancement of bed shear stress produced by the interaction of the supercritical stream with bed corrugations.

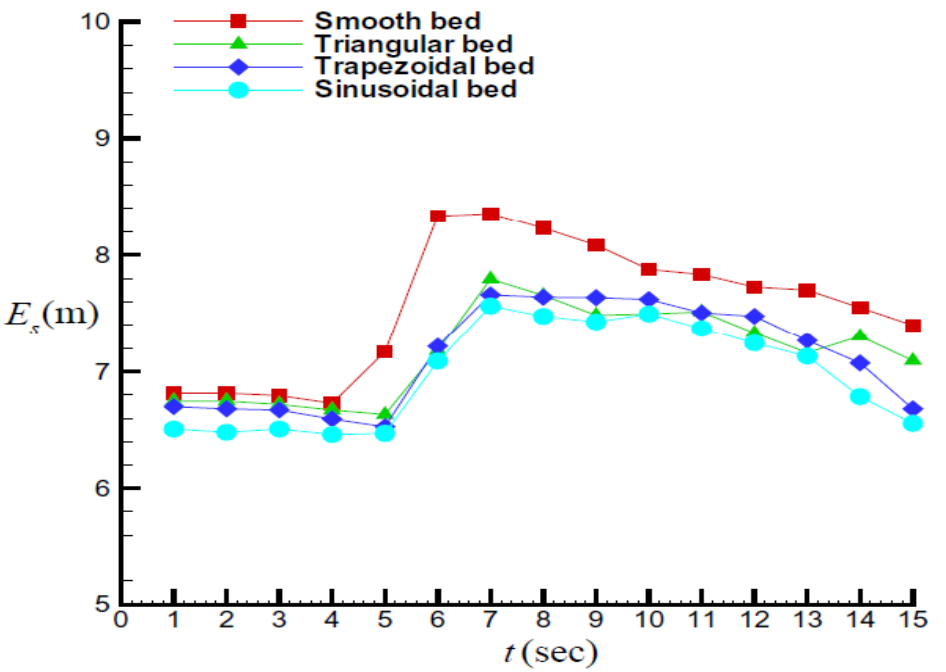

Fig 7. Time histories of energy specific for different beds at $F_1 = 1.7$ and x = 100 m.

The effect of different corrugated beds on vorticity is also shown in Fig. 8. It shows that the high vorticity area for the sinusoidal bed is larger than that for the smooth, triangular, and trapezoidal beds as shown in the circulated regions. This is because the interaction of the supercritical stream with bed corrugation produces a high vorticity level. Hydraulic jumps are in general associated with high vorticity production by energy dissipation, see [33].

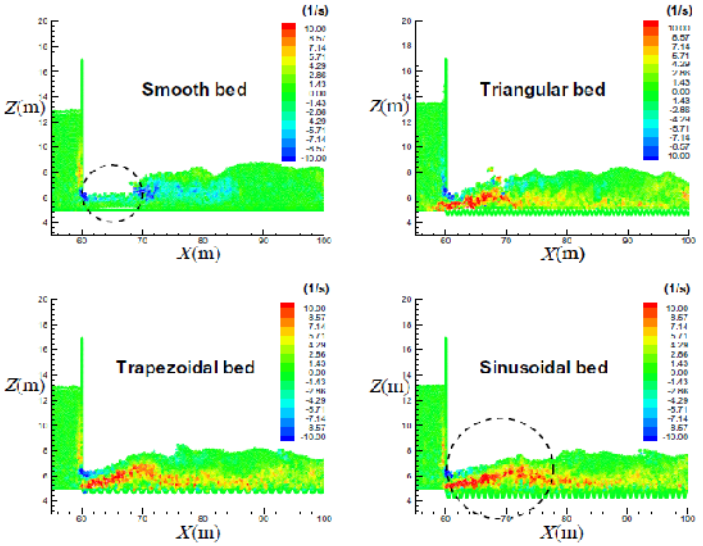

Fig 8 Surface profiles and vorticity contours for different beds at $F_1 = 1.7$ and t = 6.0 sec.

Summary

In the present study, a SPH model has been established to simulate characteristics of the hydraulic jump in a corrugated bed. Four models including a smooth, a triangular, a trapezoidal, and sinusoidal beds have been considered to study the effect of corrugation on a hydraulic jump. Variations of the hydraulic jump due to different corrugations have been successfully predicted by the proposed SPH model. The energy dissipation in a hydraulic jump is calculated as well. In terms of numerical results, it turns out that a corrugated bed can dissipate more energy in a hydraulic jump than a smooth bed. Among those three corrugated beds, the sinusoidal bed has the highest energy dissipation in a hydraulic jump. In conclusion, this study may provide useful information and a useful tool for an engineer who would like to design a corrugated bed to avoid the damage resulting from a hydraulic jump in a channel.

Acknowledgments

The authors would like to express their gratitude for the support given by National Science Council Taiwan (Project No.: NSC 99-2212-E-011-041-MY3). The authors are grateful to Dr. Benedict Rogers, Prof. O.M. Faltinsen, Dr. A. Calogrossi, Dr. Shan Zou, Dr. Rui Xiu, and Dr. Shao for their helpful discussion as well.

Nomenclature

A	:A continuous function.
B	:A constant related to the bulk modulus of elasticity of the fluid.
$\bar{c}$	:Average speed of sound of particles, m/s
dx	:particle spacing in x-direction, m
dz	:particle spacing in z-direction, m
g	:Gravitational acceleration, m/s^2
h	:Smoothing length, m
m	:Mass, kg
n	:Normal direction.
P	:Pressure, Pa
q	:Non-dimensional distance between particles.
r	:Displacement, m
v	:Velocity, m/s
w	:The kernel function.

Greek symbol

α :Constant related to the dimensional space.
β :Correction vector.
γ :The polytrophic constant.
ε :XSPH correction.
μ :Dynamic viscosity of particle, kg/(m s)
υ :Kinematic viscosity, m^2/s
$\mathbf{\Pi}$:Viscosity term.
$\bar{\rho}$:Average density of particles, kg/m^3
τ :Stress tensor of particle, $kg/(ms^2)$

Subscripts

a, b :particle identity.

References

[1] A. Abbaspour, D. Farsadizadeh, A. H. Dalir, A.H., and A. A. Sadraddini, Numerical study of hydraulic jumps on corrugated beds using turbulence models, Turkish Journal of Engineering Environtmental Science. 33(1), (2009) 61-72.

[2] J. Bonet, and T. S. Lok, Variational and momentum preservation aspects of smooth particle hydrodynamic formulations, Computer Methods in Applied Mechanics and Engineering. 180(1), (1999), 97-115.

[3] Bureau of Reclamation, U.S. Research studies on stilling basins, energy dissipators, and associated appurtenances.Hydraulic Lab. Report Hyd.399. USA, (1955).

[4] H. Chanson, The hydarulics of open channel flow : an introduction. Butterworth-Heinemann. 2nd edition. UK, (2004).

[5] T. Capone, A. Panizzo, C. Cecioni, and R. A. Dalrymple, Accuracy and stability of numerical schemes in SPH, Proceedings of SPHERIC Second International Workshop, Madrid, Spain, (2007).

[6] T. J. Chang, H. M. Kao, K. H. Chang, and M. H. Hsu, Numerical simulation of shallow-water dam break flows in open channels using smoothed particle hydrodynamics, Journal of Hydrology. 408, (2011), 78-90.

[7] C. R. Chu, and H. M. Tseng, A two dimensional TVD scheme for unsteady open channel flows simulation. XXIX IAHR Congress, Sept.16-21, Beijing, China, (2001).

[8] A.Colagrossi, A meshless lagrangian method for free surface and interface flows with fragmentation, Ph.D. thesis. Department of Mechanical Engineering, University of Rome, Italy, (2003).

[9] A. Colagrossi, and M. Landrini, Numerical simulation of interfacial flows by smoothed particle hydrodynamics, Journal of Computational Physics. 191(2), (2003), 448-475.

[10] A. J. C. Crespo, M. Gomez-Gesteira, and R. A. Dalrymple, Boundary conditions generated by dynamic particles in SPH methods, CMC:Computers, Materials, and Continua. 5(3), (2007), 173-184.

[11] R. A. Dalrymple, and B. D. Rogers, Numerical modeling of water waves with the SPH method, Coastal Engineering. 53(2), (2006), 141-147.

[12] L. Delorme, A. Colagrossi, A. Souto-Iglesias, R. Zamora-Rodrguez, and E. Bota-Vera, A set of canonical problems in sloshing. Part I: Pressure field in forced roll-comparison between experimental results and SPH. Ocean Engineering. 36(2), (2009), 168−178.

[13] G. Dilts, Moving-least-squares-particle hydrodynamics-I. consistency and stability, International Journal for Numerical Methods in Engineering. 44(8), (1999), 1115-1155.

[14] S. A. Ead, and N. Rajaratnam, Hydraulic jumps on corrugated beds, J. of Hyd. Eng., ASCE. 128, (2002), 656-663.

[15] S. A. Ead, N. Rajaratnam, C. Katopodis, and F. Ade, Turbulent open-channel flow in circular corrugated culverts, J. of Hyd. Eng., ASCE. 126, (2000), 750-757.

[16] I. H. Elsebaie, S. Shabayek, Formation of hydraulic jumps on corrugated beds, International Journal of Civil & Environtmental Engineering IJCEE-IJENS. 10(1), (2010), 40-54.

[17] I. Federico, S. Marrone, A. Colagrossi, F. Aristodemo, and M. Antuono, Simulating 2D open-channel flows through a SPH model, European Journal of MechanicsB/Fluids. doi:10.1016/j.euromechflu.2012.02.002, (2012).

[18] A. M. Gharangik, and M. H. Chaudhry, Numerical simulation of hydraulic jump, J. of Hyd. Eng., ASCE. 117, (1991), 1195-1209.

[19] H. Gotoh, T. Shibahara, and T. Sakai, Sub-particle-scale turbulence model for the MPS method-Lagrangian flow model for hydraulic engineering, Advanced Methods for Computational Fluid Dynamics. 9(4), (2001), 339-347.

[20] A. Khayyer, and H. Gotoh, Development of CMPS method for accurate water surface tracking in breaking waves, Coastal Engineering Journal. 50(2), (2008). 179-207.

[21] G. R. Liu, and M. B. Liu, Smoothed particle hydrodynamics: a meshfree particle method, World Scientific Publishing Co. Pte. Ltd., Singapore, (2003).

[22] D. Lopez, R. Marivela, and L. Garrote, Smoothed particle hydrodynamics model applied to hydraulic structures:a hydraulic jump test case, Journal of Hydraulic Research. 48(1), (2010), 142-158.

[23] J. J. Monaghan, Smoothed particle hydrodynamics, Annual Reviews Astronomy and Astrophysics, 30(1), (1992), 543-574.

[24] J. J. Monaghan, and A. Kos, Solitary waves on a cretan beach, Journal of Waterway, Port, Coastal, and Ocean Engineering. 125(3), (1999), 145-154.

[25] J. J. Monaghan, A. Kos, and N. Issa, Fluid motion generated by impact, Journal of Waterway, Port, Coastal, and Ocean Engineering. 129(6), (2003), 250-259.

[26] J. P. Morris, P. J. Fox, and Y. Zhu, Modeling lower reynolds number incompressible flows using SPH, Journal of Computational Physics. 136(1), (1997), 214-226.

[27] B. R. Munson, D. F. Young, and T. H. Okiishi,Foundamental of fluid mechanics, John Wiley & Son. Fourth Edition. USA, (2002).

[28] M. Narayanaswamy, A. J. C. Crespo, G. M. Gesteira, and R. A. Dalrymple,R.A, SPHysics-FUNWAVE hybrid model for coastal wave propagation, J. Hydraul. Res. 48, (2010), 85-93.

[29] S. Nikmehr, and A. Tabebordbar, Hydraulic jumps on adverse slope in two cases of rough and smooth bed, Research Journal of Applied Sciences Engineering and Technology. Netherlands, 2(2), (1995), 19-22. .

[30] A. Panizzo, Physical and numerical modelling of sub-aerial landslide generated waves." Ph.D. thesis. Department of Civil Engineering, Universita degli studi di L'Aquila, L'Aquila, Italy, (2004).

[31] C. S. Peskin, Numerical analysis of blood flow in the heart, Journal of Computational Physics. 25(3), (1977), 220-252.